A virtual EXV mass flow sensor for applications with two-phase flow inlet conditions

Christian K. Bach*, Eckhard A. Groll, James E. Braun

Ray W. Herrick Laboratories, Purdue University, West Lafayette, IN, USA

*Corresponding Author: bachc@purdue.edu

ABSTRACT

In conventional vapor compression systems, electronic expansion valves (EXVs) are used for refrigerant flow control. Subcooled refrigerant enters the expansion device and is expanded to the evaporation pressure while the valve opening is modified to achieve the desired mass flowrate. The relationship between the inlet and outlet conditions, the opening, and the mass flowrate has been extensively studied, e.g. by Park et al. (2007) and appropriate empirical correlations have been developed. However, for certain operating conditions (e.g. low refrigerant charge) or applications that generally have two-phase inlet conditions (e.g. balancing valves used in a hybrid control scheme as proposed by Kim et al. (2008)), these correlations are not applicable, since even low inlet vapor fractions lead to a significant reduction of the valve mass flowrate at a given opening.

This paper proposes a continuous correlation that can be used for both two-phase and subcooled valve inlet conditions. The benefit of the continuity is that there is a smooth transition between subcooled and two-phase inlet conditions, which is essential for control and simulation purposes. The new correlation employs the Buckingham-Pi theorem as proposed by Buckingham (1914). The selected dimensionless Pi-groups describe opening of the valve, subcooling, inlet and outlet pressures, driving pressure difference across the valve, inlet density, surface tension, and viscosity.

The data that was used to determine the coefficients of the correlation was taken on a dedicated valve test stand, which was sized for the per-circuit capacity of a typical 5-ton R410A heat pump and a 3-ton R404A large room cooling system. The purpose of these tests was mainly to map the valves for the low pressure drops, high inlet qualities and large valve openings that occur when they are used as balancing valves in a hybrid control approach. Two commercially available valves of different rated capacity were tested. Due to the much higher valve capacity for subcooled inlet conditions, valve openings of less than 5% occurred in that case. This led to an accuracy of the correlation for these points that is less than what typically can be found for correlations with subcooled inlet conditions in the open literature. However, for two-phase flow inlet conditions, the resulting RMS of 1.0 g/s for the 8-PI correlation is sufficiently small to use the approach for estimating the refrigerant mass flow and using the EXV as a virtual flow sensor.

The limitations of this approach in practical applications, as well as possible applications in fault detection and diagnostics are shown for application as balancing valves within a 5-ton R410A heat pump and a 3-ton R404A large room cooling system.

1. INTRODUCTION

The hybrid control for evaporators was proposed by Kim et al. (2008) to significantly reduce the performance degradation caused by air-side and refrigerant-side maldistribution. In the hybrid control approach, as shown in Figure 1, balancing valves are inserted into the feeder lines for the individual circuits after the refrigerant distributor. The main pressure drop is achieved with the primary expansion valve while the secondary valves only provide a small pressure drop. These valves may have a limited actuation range, which might make them cheaper to manufacture than smaller capacity individual circuit expansion valves.

The main intent of the hybrid control is to provide individual circuit flow control. If air-side maldistribution is applied to the evaporator, the resulting flowrates for the circuits will differ. If an electronic valve type is chosen as the balancing valve, e.g. a stepper valve, then the opening degree of the valves can be used to determine the flowrate into each individual circuit. Unfortunately, the inlet to the expansion valves is in two-phase condition, which means that there was no correlation available to determine this flowrate.

The purpose of this paper is to show a correlation that can be used to determine the flowrate through the individual circuits by using the balancing valves. This correlation makes it possible to use EXVs with two-phase and subcooled inlet conditions as a virtual flow sensor.

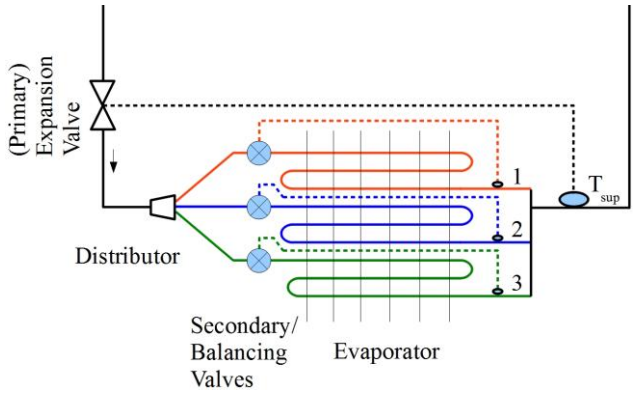

Figure 1: Hybrid control approach for 3-circuit evaporator

2. Test setup and testing

2.1 Test setup

Figure 2 shows a simplified schematic of the test stand. The test stand is designed as a standard refrigeration cycle modified with two expansion branches and an electric reheater for additional control of the subcooling. The test branch, 7, uses a primary expansion valve to adjust the inlet pressure to the secondary valve 10, which is the valve to be tested. The ¼'' (6.35 mm) connection line 9 between the two valves has a straight section of 0.3 m before the valve inlet to allow for the two-phase flow to develop. The effort to install in-flow measurements for up to 9 circuits in typical outdoor heat exchangers of 5-ton heat pump systems will likely not be justifiable. Therefore, a surface measurement was used to determine the inlet temperature as shown in Figure 3. This allows for the determination of the performance of the valve as a function of the cheaply to obtain surface temperature at the inlet. The temperature measurement of the primary expansion valve, type EXL B0B was done in the same manner.

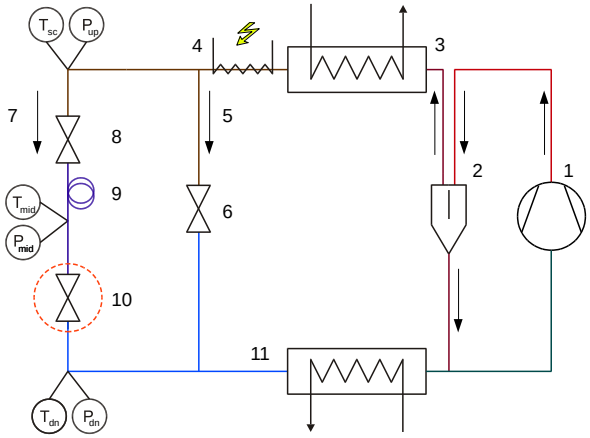

Description

1) Compressor
2) Oil separator
3) Condenser, followed by electric heater
4) Electric heater
5) Bypass path
6) Bypass valve(s)
7) Test path
8) Primary EXV
9) Connection line
10) Secondary/ Balancing EXV
11) Evaporator

Figure 2: Simplified schematic of test stand

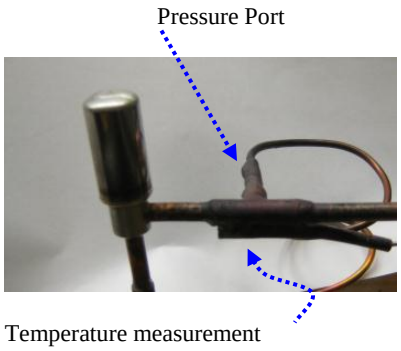

Figure 3: Measurements at valve inlet

2.2 Test plan

Figure 4 shows the hybrid expansion process and directions of change for the inlet conditions to the balancing valve for a fixed evaporation pressure under two-phase inlet conditions. In addition, changing operating conditions lead to a changing compressor capacity and result in different evaporation temperatures and required mass flowrates through the valve. The required individual circuit mass flowrate in the hybrid control scheme is furthermore influenced by air-side maldistribution. From these considerations, the following variables can be adjusted within limits to obtain a certain valve opening:

1) Subcooling (only for subcooled inlet conditions to balancing valve),

2) Inlet enthalpy (only for two-phase inlet conditions),
3) Inlet pressure of balancing valve,
4) Outlet pressure of balancing valve,
5) Mass flow rate.

To capture possible nonlinear effects, 3 points in each direction were considered in the initial test plan. As a result, for each subcooled and two-phase inlet condition, $3^4 = 81$ points are theoretically needed. Due to the limitations of the valve in terms of resolution for small openings (subcooled inlet conditions) and maximum opening (low pressure drop tests), some of the points had to be skipped. The tests were initially conducted with R404A as the refrigerant. Additional tests were conducted with R410A, where 2 instead of 3 different target mass flow rates were used, e.g. the smallest target mass flow rate was dropped. The tests that were used to develop the correlations were conducted over the ranges of operating conditions shown in Table 1 and Table 2 for subcooled and two-phase inlet conditions, respectively. It is recommended that the presented correlations only be used within the limits shown in these tables.

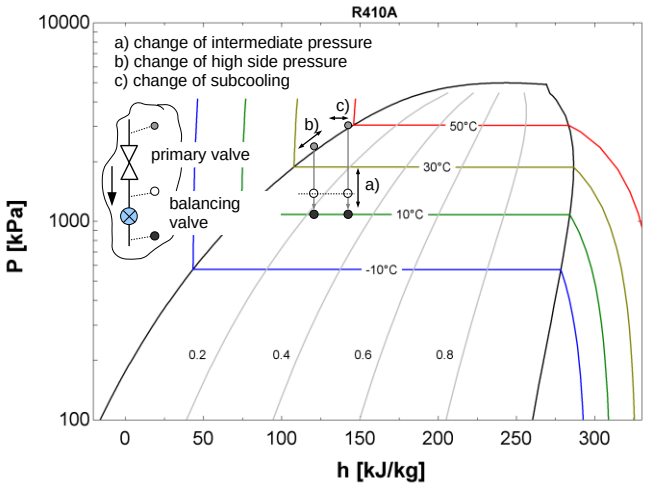

Figure 4: Hybrid expansion process in Log(p)-h plot

Table 1: Range of tested values, subcooled inlet conditions, B0B (B1F) Valve

Property	min - R404A	max - R404A	min - R410A	max - R410A
Inlet pressure [kPa]	963 (977)	2874 (2466)	1560 (1301)	3112 (3053)
Inlet subcooling [K]	1.8 (1.2)	20.5 (15.8)	0.8 (1.2)	16.7 (15.6)
Outlet pressure [kPa]	248 (245)	532 (531)	359 (355)	1220 (1208)
Pressure drop PI_{14} [-]	0.117 (0.493)	0.630 (0.896)	0.374 (0.142)	0.846 (0.840)
Mass flowrate [g/s]	1.7 (1.7)	22.2 (23.4)	5.1 (3.9)	22.7 (23.8)

Table 2: Range of tested values, two-phase inlet conditions, B0B (B1F) Valve

Property	min - R404A	max - R404A	min - R410A	max - R410A
Inlet pressure [kPa]	333 (341)	2341 (2466)	583 (426)	1942 (2029)
Inlet enthalpy [kJ/kg]	33.9 (28.9)	130 (134)	43.2 (30.5)	172 (112)
Outlet pressure [kPa]	249 (245)	528 (524)	357 (357)	1200 (1184)
Pressure drop PI_{14} [-]	0.227 (0.158)	0.848 (0.860)	0.044 (0.063)	0.793 (0.741)
Mass flowrate [g/s]	1.6 (1.7)	16.3 (22.8)	4.1 (4.0)	22.8 (23.8)

Table 3: Number of training pionts

Test series	Number of training points	Test series	Number of training points
B0B – R410A	52	B1F – R410A	23
B0B – R404A	24	B1F – R404A	20

2.3 Limitations of stepper expansion valves as virtual flow sensors

Expansion valves with stepper motors do not have a transducer for their current position. To determine their needle position, the number of steps that the valve moved has to be used instead. This requires an initial zeroing of the valve: the valve is moved to the closed position by a larger number of steps than the spindle moving the needle is

physically long. At some point, the needle hits the orifice. At this point, the magnetic field of the stator twists the needle until the force due to torque is equal to the magnetic field force. At that point, the magnetic stator starts slipping over the magnetic rotor until the field polarities are opposite. The result is a snapping noise, since the needle rotates backwards. Moving back from that point, the approximate needle opening position is known. Emerson (2008) specifies that the valve starts to open at 32±20 steps. Since the rated total number of pulses is 500, this provides a significant source of error. For the valve testing, the actual opening position of the valves was determined in a trial and error procedure using the coriolis mass flow meter in the test stand. The resulting opening position is conservatively considered to be within ±2 steps. In practical applications, the opening position might be found using the evaporation pressure and/or temperature during standstill periods of the system – with reduced accuracy. Another small source of error is hysteresis caused by mechanical friction of the spindle. In case of the smaller B0B valve, this friction was barely noticeable, while it was an issue for the subcooled points of the B1F valve: for some test points, the hysteresis was used as an "intermediate step" to obtain the required mass flowrate. Another limitation is possible fouling of the valve, the most significant problem likely being small metal chips that are caused by poor field installation practices or loose sealing material from threaded connections. Therefore, a flushing procedure should be included in the controls, where the valve is periodically fully opened for a short period of time.

3. Data evaluation

3.1 Approach

The exact behavior of two-phase flow in expansion valves is still not very well understood. As a result, correlations for single-phase inlet conditions are empirical. The same is applicable for correlations that are used to describe the mass flowrate through short tube orifices, which sometimes include two-phase inlet conditions (e.g. Payne and O'Neil, 2004 or Choi *et al.*, 2004). As a result, it was decided to start from the approach chosen by Choi *et al.* (2004). The authors used the Buckingham (1914) PI-theorem. The resulting general form to obtain the PI_1 group, which is the dimensionless mass flow rate, is shown in Equation (1). Since expansion valves were used in this study, rather than short tube orifices, Choi's PI groups had to be modified. Recalling the results of Shanwei *et al.* (2005), it is assumed that the mass flow rate is independent of the needle geometry. The diameter, D, in Choi's PI_6-group is therefore replaced by the step number, S, as a measure of the relative cross sectional area. The length, L, in the same group is replaced by the fully open step number S0. For the PI_1 group, which represents the mass flow rate, the constant orifice diameter of the valve is used as the diameter, to retain information about the valve size. A total of 16 possible PI groups were tested for significance. These groups also included pressure drop, since choked flow is not applicable for some of the small pressure drop test points. Table 4 shows the PI groups that were used in the final correlations. To make sure that the model works for all inlet conditions, it was necessary to ensure continuity of all groups. The group $PI_{5,K}$, which represents the subcooling, is defined with an offset of 273.15 K in the numerator. Some groups, e.g. PI_{13} through PI_{15} have overlapping meaning. It was found that their concurrent usage led to an improvement of the fit. The two main reasons for that are a) flow conditions were always considered to be non-choked, which is not always the case and b) a larger number of coefficients means a better fit to the data–which always will have measurement error, especially if inlet quality is calculated based on on-surface subcooling measurement. As a result of b), it is not favorable to use an excessively large number of coefficients for a finite set of data points.

$$PI_1 = c_0 \cdot PI_2 \cdot PI_3 \cdot .... \cdot PI_n = \frac{\dot{m}_{kg}}{D_{orifice}^2 \cdot \sqrt{\rho_f \cdot P_{mid}}} \tag{1}$$

Table 4: PI groups considered for correlations

PI Group	Represented property
$PI_1 = \frac{\dot{m}_{kg}}{D_{orifice}^2 \cdot \sqrt{\rho_f \cdot P_{mid}}}$	Mass flowrate
$PI_3 = \frac{P_c - P_{down}}{P_c}$	Saturation pressure at valve outlet
$PI_4 = \frac{P_c - P_{sat}}{P_c}$	Saturation pressure at valve inlet

PI Group	Represented property
$PI_{5,K} = \frac{\text{ConvertTemp}(C, K, \Delta T_{sub})}{\text{ConvertTemp}(C, K, T_c)}$	Subcooling at inlet to balancing valve (continuous)
$PI_6 = \frac{S_0}{S}$	Valve opening
$PI_7 = \frac{\rho_f}{\rho_g}$	Density ratio (inlet)
$PI_8 = \frac{\mu_f - \mu_g}{\mu_g}$	Viscosity difference at inlet
$PI_9 = \frac{\sigma}{S \cdot P_{mid}}$	Surface tension at inlet
$PI_{12} = \frac{\rho_{mean}}{\rho_f}$	Inlet density
$PI_{13} = \frac{P_{mid} - P_{dn}}{P_c}$ $PI_{14} = \frac{P_{mid} - P_{dn}}{P_{mid}}$ $PI_{15} = \frac{P_{mid} - P_{dn}}{P_{dn}}$	Relative pressure difference

Note: Pressures for PI groups are given in Pa; only PI groups used in final correlations are shown

3.2 Continuous correlations for individual valves and refrigerants

Starting out with a correlation using 17 PI groups, the number of PI groups was reduced to 9 without major loss of accuracy. Starting from this correlation, half the data points were selected based on a random seed to determine the coefficients of the correlation. The coefficients for the PI groups were found by reducing the mean square error of the set of data points given for the difference between correlated and measured PI_1 group. This group, as shown in Equation (1), represents the mass flow rate. In the denominator, the square root of the inlet pressure to the secondary valve, p_{mid} is contained. This leads to a partial normalization of the mass flow rate, such that values taken with higher inlet pressure have similar importance for the determination of the coefficients as the values taken at smaller inlet pressures. By that, the coefficients with lower mass flowrates gain in importance for finding the coefficients. In addition to this correlation, a further reduction to 8, 7, 6, and 5 PI groups was done. The following correlations resulted from this process:

5 PI continuous: $$PI_1 = c_0 \cdot PI_3^{c_3} \cdot PI_{5,K}^{c_{5,K}} \cdot PI_6^{c_6} \cdot PI_{12}^{c_{12}} \cdot PI_{14}^{c_{14}}, \quad (2)$$

6 PI continuous: $$PI_1 = c_0 \cdot PI_4^{c_4} \cdot PI_{5,K}^{c_{5,K}} \cdot PI_6^{c_6} \cdot PI_{12}^{c_{12}} \cdot PI_{14}^{c_{14}} \cdot PI_{15}^{c_{15}}, \quad (3)$$

7 PI continuous: $$PI_1 = c_0 \cdot PI_4^{c_4} \cdot PI_{5.K}^{c_{5,K}} \cdot PI_6^{c_6} \cdot PI_8^{c_8} \cdot PI_{12}^{c_{12}} \cdot PI_{14}^{c_{14}} \cdot PI_{15}^{c_{15}}, \quad (4)$$

8 PI continuous: $$PI_1 = c_0 \cdot PI_4^{c_4} \cdot PI_{5.K}^{c_5} \cdot PI_6^{c_6} \cdot PI_8^{c_8} \cdot PI_9^{c_9} \cdot PI_{12}^{c_{12}} \cdot PI_{14}^{c_{14}} \cdot PI_{15}^{c_{15}} \quad (5)$$

9 PI continuous: $$PI_1 = c_0 \cdot PI_4^{c_4} \cdot PI_6^{c_6} \cdot PI_7^{c_7} \cdot PI_8^{c_8} \cdot PI_9^{c_9} \cdot PI_{12}^{c_{12}} \cdot PI_{13}^{c_{13}} \cdot PI_{14}^{c_{14}} \cdot PI_{15}^{c_{15}}. \quad (6)$$

Equation (6) does not contain a term for the subcooling, which might be an indication that the data was fit to the measurement points in a way that did not have a profound physical meaning or that the subcooling gained as a result of conduction between high- and low temperature sides through the valve body was the dominating effect. Conduction effects are not important in standard EXV applications, where the flowrates are much higher. Figure 5 shows the deviation $\Delta\dot{m}$, defined as

$$\Delta\dot{m} = \dot{m}_{correl} - \dot{m}_{mess} \tag{7}$$

for the measured data points with R404A as a function of measured mass flowrate for the 5 different correlations. Overall, the reduction in accuracy for the correlations with fewer coefficients is relatively small for both valves. Figure 5 b) shows more deviation for the larger B1F valve than for the smaller B0B valve (Figure 5 a). One of the reasons for this behavior can be found in Figure 6 a) and b). While the data points for the B0B valves are spread over the opening range with concentration of points at full opening and 1/5 of full opening, the points for the larger B1F valve are concentrated below 1/10 of the full valve opening. This leads to an increased influence of hysteresis and valve zero position accuracy on the result. Additionally, due to the larger valve body and tube diameter, conduction through the valve to the surface mount thermocouples led to a larger measurement error and an increase of the effective subcooling before the valve orifice, especially at lower flowrates.

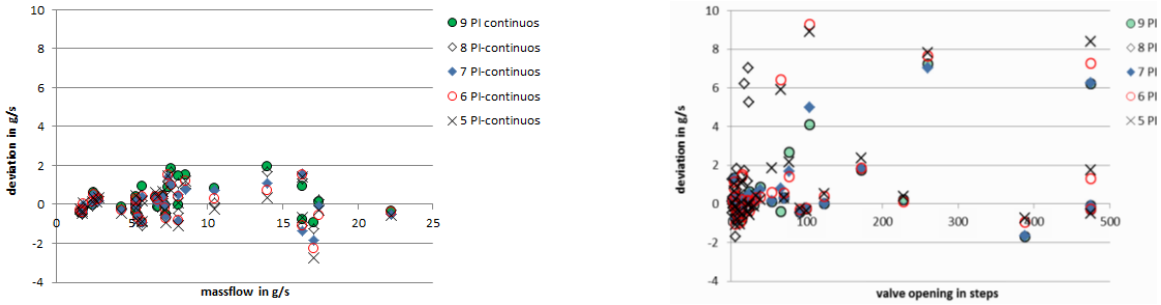

a) B0B Valve b) B1F Valve

Figure 5: Continuous correlations for R404A, deviation as a function of mass flowrate

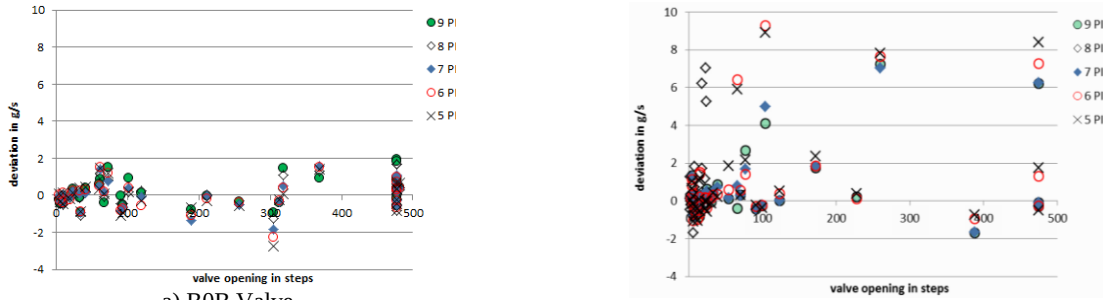

a) B0B Valve b) B1F Valve

Figure 6: Continuous correlations for R404A, deviation as a function of opening degree

Figure 7 shows the result for the R410A data. For both valves and all correlations, most of the mass flow rates are predicted within a span of ±2 g/s.

a) B0B Valve b) B1F Valve

Figure 7: Continuous correlations for R410A, deviation as a function of opening degree

3.3 General continuous correlations for both valves and refrigerants

To check whether the principle approach of the chosen correlations is correct, randomly chosen points of the two tested valves and refrigerants from Section 3.2 were chosen and a new set of coefficients for Equations (2) through (6) were determined. It was found that the accuracy of the correlations increases slightly with the number of PI groups, starting from an RMSE of 1.2 g/s with 5 PI groups and ending with an RMSE of 1.0 g/s for the 8 and 9 PI group correlations for the entire set of data points. Table 5 shows the coefficients for the correlations together with their accuracy. The 9 PI group correlation is not recommended, since it does not contain a subcooling term and might therefore be inaccurate for larger subcooling values. Figure 8 shows the accuracy in the classical form. In the range of 10 to 35 g/s, the 8 PI group correlation predicts most of the points within a ±15 % error. Due to the issues associated with small mass flow rates, their percentage deviation is larger. Figure 8 b) shows the results for the 8 PI group correlation in the previously chosen format. A minor trend to under prediction of larger mass flow rates can be noticed for the B0B valve. This might be caused by the unknown needle geometry. The accuracy for the B1F valve with R404A increased compared to the individual B1F-R404A correlation, which suggests that the randomly selected half points for that valve were not a good choice for finding coefficients.

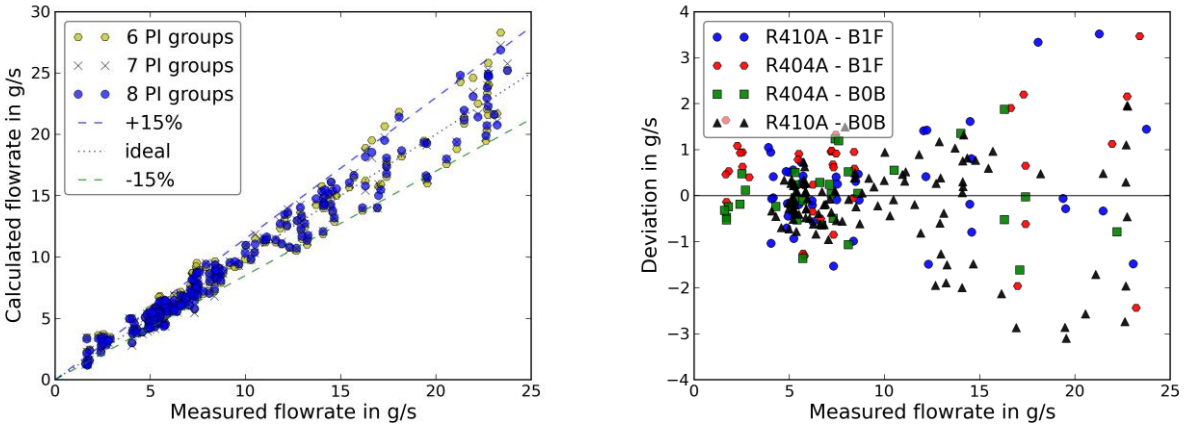

a) Predicted and measured flowrate b) deviation, 8 PI group correlation

Figure 8: Measured and predicted flowrate, both valves and refrigerant

Table 5: Coefficients and statistics of correlations

	Correlation type				
c_n	**5 PI**	**6 PI**	**7 PI**	**8 PI**	**9PI**
0	1.775614194	2.439128478	3.200235283	861.7726414	5.426487251e+23
3	-0.5678193369	0	0	0	0
4	0	0.01782559397	0.4065298029	0.04838726475	-2.303134246
5,K	6.590248312	6.347449717	4.441794839	4.519479258	0
6	-0.6876234976	-0.6762577243	-0.6852101108	-0.893741257	-2.702032769
7	0	0	0	0	-0.9465847683
8	0	0	-0.268902318	-0.4749436201	-0.007100161791
9	0	0	0	0.2053180637	2.013175541
12	0.4933574114	0.5414994269	0.5282836841	0.5531117265	0.5494573332
13	0	0	0	0	1.585712705
14	0.1971396137	0.4910193858	0.464122395	0.48053314	-1.115615678*
15	0	-0.2009067249	-0.1740114354	-0.1795276583	-0.1730842306
RMS	1.18 g/s	1.13 g/s	1.05 g/s	1.01 g/s	1.00 g/s
BIAS	-0.05 g/s	0.02 g/s	0.03 g/s	0.02 g/s	0.01 g/s
MIN	-3.56 g/s	-3.56 g/s	-3.25 g/s	-3.10 g/s	-2.94 g/s
MAX	4.52 g/s	4.89 g/s	3.84 g/s	3.52 g/s	3.53 g/s

3.4 Continuous correlations applied to data from a 3-ton large room cooling system evaporator coil

In the next step, the continuous 8 PI group correlation was applied to data that was taken with a 3-ton large room cooling system equipped with a hybrid control scheme. B1F valves were used as balancing valves. The coil had 8 circuits of equal length and similar layout. Saturated inlet temperature to the valves was measured before the distributor, and the outlet temperature was measured for each valve individually. Based on the behavior of the system during testing, it was found that the quality maldistribution of the distributor changes with opening position of the balancing valves. To illustrate this issue, the large room cooling system was operated with hybrid control and then additionally with primary expansion valve (PEXV) fully open to prevent quality maldistribution in the distributor. Figure 9 a) shows the result for the clean coil tests. While, for the PEXV open tests, the individual circuit flowrates are very evenly distributed, this is not the case for the two-phase inlet conditions: circuits 1 and 7 predict less than average, while circuit 8 predicts more than average mass flow rates. Since the individual circuit mass flow rates were controlled to achieve equal exit superheats, the mass flow rates should be very similar. The difference in predictions is therefore a result of smaller than average inlet qualities to valves 1 and 7 and larger than average quality to valve 8. Figure 9 b) shows the results for 2/3 of the face area blocked. The predicted flowrates for both tests are the same within the measurement tolerance. The predicted mass flow rates for the PEXV open test have a larger error than the ones in subfigure a). The reason for this difference is that the valve opening positions were calibrated for the results shown in subfigure a) while they were not calibrated for the results shown in subfigure b). Therefore, the manufacturer's data was taken for the accuracy of the opening position. This illustrates that the usefulness of the EXV as virtual flow sensor is limited for small valve openings, as they occur with oversized valves under subcooled inlet conditions. The average individual circuit flowrates for the PEXV open tests are over predicted by 15.6% for the clean coil and 8.3% for the blocked coil tests. This is likely caused by a minor amount of flashing in the primary expansion valve in addition to the limited of the accuracy of the correlation and its application.

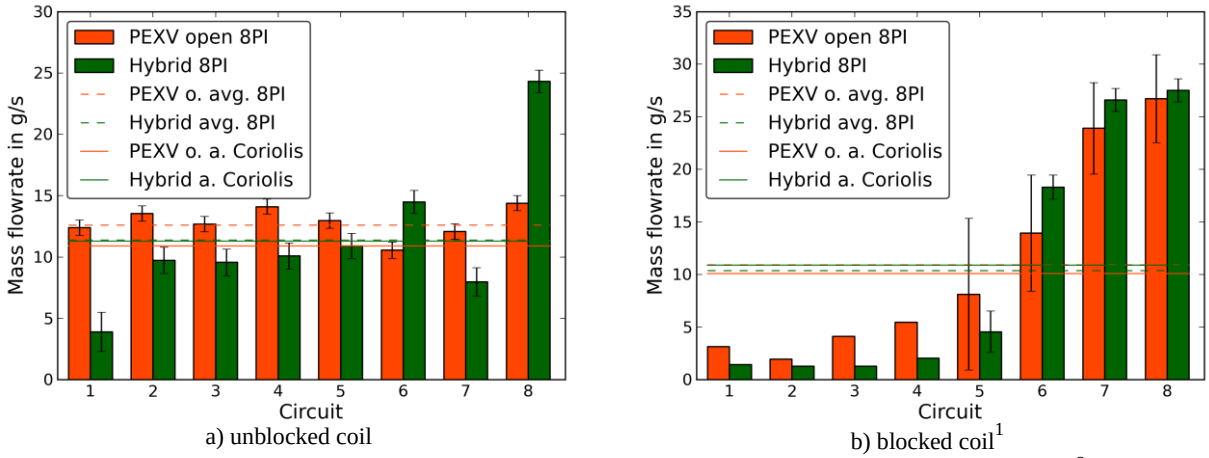

a) unblocked coil b) blocked coil[1]

Figure 9: Measured average and predicted flowrates, large room cooling system[2] for 2°C room temperature and 46°C ambient temperature

3.5 Continuous correlations applied to data from a 5-ton domestic heat pump

Similar tests as for the 3-ton large room cooling system were conducted for a 5-ton domestic heat pump in heat pump mode with the hybrid control scheme. B0B valves were used as balancing valves for the 9 circuits of the outdoor heat exchanger. The two top and bottom circuits had 10 tubes while the remaining

[1] Error bar for circuits 1 through 4 not given, since lower value less than 0.

[2] Error bars based on measurement accuracy, PI_1 RMS of correlation and valve opening position accuracy. ±2 steps for PEXV open for unblocked coil, else ±20 steps accuracy.

circuits had 8 tubes. A smaller primary expansion valve was used, which resulted in two-phase inlet conditions, even if the valve was fully opened. Inlet pressure to the balancing valves was measured before the distributor, and the exit temperature of the first balancing valve was used for all circuits. During the testing, it was found that quality maldistribution occurs, which was also suggested by the predicted unblocked coil mass flow rates, as shown in Figure 10 a). The predicted mass flow rates of some circuits differ by more than the predicted error between the hybrid and primary valve fully open tests. All circuits except circuit 7 had very similar refrigerant side coil surface usage. Circuit 7 had a better refrigerant side coil surface usage for the PEXV open case. For the blocked coil cases, as shown in Figure 10 b), the differences between the two mass flow rate predictions are within the measurement error.

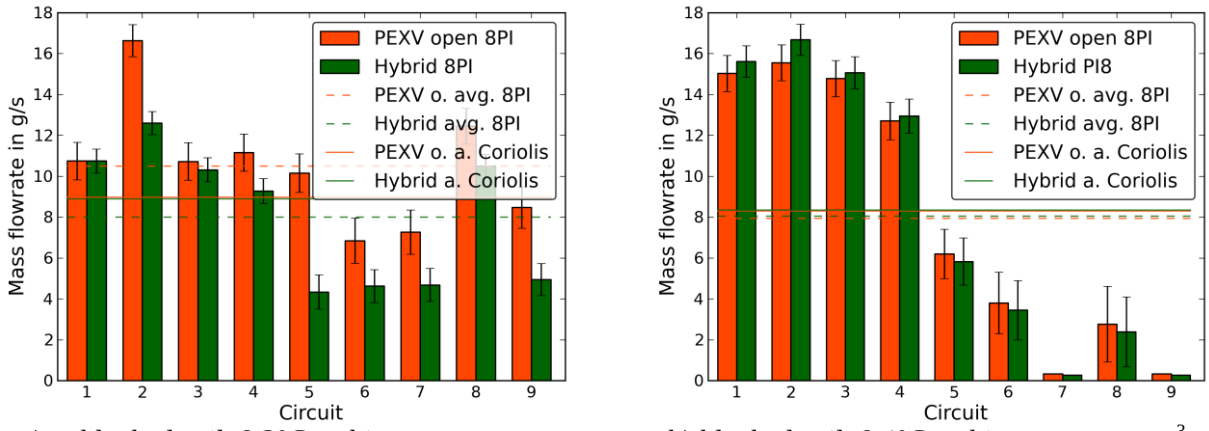

a) unblocked coil, 8.3°C ambient temperature b) blocked coil, 8.4°C ambient temperature[3]

Figure 10: Measured average and predicted flowrates, domestic heat pump[4] for 21.1°C return temperature

3.6 Possible applications for system operation, fault detection and diagnosis

The detected individual circuit mass flow rates can be used to determine the need for defrost or coil cleaning. An algorithm could evaluate the change of the relative mass flow rates over time to detect decreasing capacity of individual circuits. If more than e.g. 2 coils show less than 50% of their initial mass flow rates, the defrost cycle or a coil cleaning request could be initiated.

6. CONCLUSIONS

A continuous 8 PI group correlation for stepper motor expansion valves was developed that allows for the valve being used as a virtual flow sensor. Coefficients for the correlation were found using two different valves and R410A as well as R404A as refrigerants. The correlation predicts most of the data points with a mass flowrate of 10 to 24 g/s taken with the original test setup within an accuracy of ±15 %. Its RMSE is 1.0 g/s for the entire set of data points.

The correlation was then used to predict the individual circuit mass flow rates of a 3-ton large room cooling system and a 5-ton domestic heat pump. In both cases, noticeable quality maldistribution in the distributor was found for clean coil conditions. For blocked coil conditions, the quality maldistribution was found to be within the measurement accuracy – which for the coils with smaller mass flow rates is larger due to smaller valve openings.

It was found that the main source of uncertainty is the valve opening position. To achieve accurate measurements, the valve opening position should therefore be calibrated.

[3] Error bar for circuits 7 and 9 not given, since lower value less than 0.
[4] Error bars based on measurement acc., PI_1 RMS of correlation and valve opening position accuracy of ±20 steps .

The proposed correlation does not consider the difference between choked and non-choked operating conditions. To get more accurate results, the correlations should therefore be split up into one for choked and one for none choked conditions.

NOMENCLATURE

Symbol	Description	Unit
D	Diameter	(m)
$\dot{m}$	Mass flowrate	(kg/s)
P	Pressure	(Pa, kPa)
PI	PI-group	(-)
S	Step number[5]	(cnst*m)
T	Temperature	(K)
v	specific volume	(m^3/kg)
x	quality	(kg_{vapor}/kg_{total})
Δ	Difference	
μ	viscosity	(kg/m-s)
ρ	density	(kg/m^3)
σ	surface tension	(N/m)

Subscripts	
0	maximum
c	critical
f, l	liquid
g	gas
in	inlet
l, f	liquid
mid	before secondary valve
out, dn	after secondary valve
sat	saturation
sc	subcooled

REFERENCES

Buckingham, E. (1914). On Physically Similar Systems; Illustrations of the Use of Dimensional Equations. *Physical Reviews*, vol, 4, p. 345-376.

Choi, J., Chung, J. T.,Kim, Y., 2004, A generalized correlation for two-phase flow of alternative refrigerants through short tube orifices, *International Journal of Refrigeration*, vol. 27, p. 393-400

Emerson Electric GmbH & Co. OHG, 2008, EXM/EXL Stepper Motor Driven Electronic Expansion Valves Technical Data, Waiblingen, Germany.

Kim, J.-H., Braun, J., Groll, E., 2008, Optimizing Refrigerant Distribution in Evaporators, ARTI Report 06040, *Herrick Labs*, Purdue University.

Park, C., Cho, H., Lee, Y., Kim, Y., 2007, Mass flow characteristics and empirical modeling of R22 and R410A flowing through electronic expansion valves, *International Journal of Refrigeration*, vol. 30, p. 1401-1407.

Payne, V., O'Neal, D., 2004, A Mass Flow Rate Correlation for Refrigerants and Refrigerant Mixtures Flowing Through Short Tubes. *HVAC&R RESEARCH*, vol. 10, p. 73-87.

Shanwei, M., Chuan, Z., Jiangping, C., Zhiujiu, C., 2005, Experimental research on refrigerant mass flow coefficient of electronic expansion valve, *Applied Thermal Engineering*, vol. 25, p. 2351-2366.

ACKNOWLEDGEMENT

The authors would like to thank the California Energy Commission, which sponsored this work under contract number PIR-08-017.

[5] The step number is linear to the spindle travel in meters.